

Exponential phase of COVID-19 expansion is driven by airport connections

Marco Tulio Pacheco Coelho ^{Corresp.,1}, **João Fabrício Mota Rodrigues** ¹, **Anderson Matos Medina** ², **Paulo Scalco** ³, **Levi Carina Terribile** ⁴, **Bruno Vilela** ², **José Alexandre Felizola Diniz-Filho** ¹, **Ricardo Dobrovolski** ²

¹ Universidade Federal de Goiás, Goiânia, GO, Brazil

² Universidade Federal da Bahia, Salvador, BA, Brazil

³ Faculdade de Administração, Economia, Ciências Contábeis (FACE), Universidade Federal de Goiás, G, GO, Brasil

⁴ Laboratório de Macroecologia, Universidade Federal de Jataí, Jataí, GO, Brasil

Corresponding Author: Marco Tulio Pacheco Coelho

Email address: marcotpchcoelho@gmail.com

The pandemic state of COVID-19 caused by the SARS CoV-2 put the world in quarantine, led to hundreds of thousands of deaths and is causing an unprecedented economic crisis. However, COVID-19 is spreading in different rates at different countries. Here, we tested the effect of three classes of predictors, i.e., socioeconomic, climatic and transport, on the rate of daily increase of COVID-19. We found that global connections, represented by countries' importance in the global air transportation network, is the main explanation for the growth rate of COVID-19 in different countries. Climate, geographic distance and socioeconomics had a milder effect in this big picture analysis. Geographic distance and climate were significant barriers in the past but were surpassed by the human engine that allowed us to colonize most of our planet land surface. Our results indicate that the current claims that the growth rate of COVID-19 may be lower in warmer and humid tropical countries should be taken very carefully, at risk to disturb well-established and effective policy of social isolation that may help to avoid higher mortality rates due to the collapse of national health systems.

1 **Exponential phase of covid19 expansion is driven by airport**

2 **connections**

3

4 Marco Túlio Pacheco Coelho¹, João Fabricio Mota Rodrigues¹, Anderson Matos
5 Medina², Paulo Scalco³, Levi Carina Terribile⁴, Bruno Vilela², José Alexandre
6 Felizola Diniz-Filho¹ & Ricardo Dobrovolski²

7

8 *1 Departamento de Ecologia, Universidade Federal de Goiás, CP 131, 74.001-970 Goiânia,*
9 *Goiás, Brazil.*

10 *2 Instituto de Biologia, Universidade Federal da Bahia, Salvador, BA, Brazil*

11 *3. Faculdade de Administração, Economia, Ciências Contábeis (FACE), Universidade Federal*
12 *de Goiás, Goiânia, Goiás, Brazil.*

13 *4. Laboratório de Macroecologia, Universidade Federal de Jataí, Jataí, GO, Brazil*

14

15

16 Corresponding Author:

17 Marco Túlio Pacheco Coelho

18 Departamento de Ecologia, Universidade Federal de Goiás, CP 131, 74.001-970 Goiânia, Goiás,
19 Brazil

20 e-mail: marcotpcoelho@gmail.com

21

22

24 Abstract

25 The pandemic state of COVID-19 caused by the SARS CoV-2, put the world in
26 quarantine, led to hundreds of thousands of deaths and is causing an unprecedented economic
27 crisis. However, COVID-19 is spreading in different rates at different countries. Here, we tested
28 the effect of three classes of predictors, i.e., socioeconomic, climatic and transport, on the rate of
29 daily increase of COVID-19. We found that global connections, represented by countries'
30 importance in the global air transportation network, is the main explanation for the growth rate of
31 COVID-19 in different countries. Climate, geographic distance and socioeconomics had a milder
32 effect in this big picture analysis. ~~Geographic distance and climate were significant barriers in~~
33 ~~the past but were surpassed by the human engine that allowed us to colonize most of our planet~~
34 ~~land surface.~~ Our results indicate that the current claims that the growth rate of COVID-19 may
35 be lower in warmer and humid tropical countries should be taken very carefully, ~~at risk to~~ disturb
36 well-established and effective policy of social isolation that may help to avoid higher mortality
37 rates due to the collapse of national health systems.

38

39

40 Introduction

41 With the worldwide spread of the novel Coronavirus Disease 2019 (COVID-19), caused
42 by the SARS-CoV-2 virus, we are experiencing a declared pandemic. One of the largest
43 preoccupations about this new virus ~~regards~~ its notable ability to spread given the absence of any
44 effective treatment, vaccine and immunity in human populations. Epidemiologists quantify the
45 ability of infectious agents to spread by estimating the basic reproduction number (R_0) statistic
46 (Delamater et al., 2019), which measures the average number of people each contagious person
47 infects. According to the World Health Organization (2020), the new coronavirus is transmitting
48 at an R_0 around 1.4-2.5, which is greater than seasonal influenza viruses that spread every year
49 around the planet (median R_0 of 1.28, Biggerstaff et al., 2014). To anticipate the timing and
50 magnitude of public interventions and mitigate the adverse consequences on public health and
51 economy, understanding the factors associated with the survival and transmission of SARS-CoV-
52 2 is urgent.

53 Because previous experimental (Lowen et al., 2007), epidemiological (Shaman et al.,
54 2010, Barreca & Shimshack 2012) and modeling (Zuk et al., 2009) studies show the critical role
55 of temperature and humidity on the survival and transmission of viruses, recent studies are
56 testing the effect of environmental variables on SARS-CoV-2 (Wang et al., 2020, Sajadi et al.,
57 2020) and forecasting monthly scenarios of the spread of the new virus based on climate
58 suitability (Araújo & Naimi 2020, *but see* Chipperfield et al., 2020). Although temperature and
59 humidity ~~are known to~~ affect the spread and survival of other coronaviruses (i.e., SARS-CoV
60 and MERS-CoV, Tan et al., 2005, Chan et al., 2011, Doremalen et al., 2013, Gaunt et al., 2010)
61 using the current occurrences of SARS-CoV-2 cases to build correlative climatic suitability

62 models without ~~taking into consideration~~ connectivity among different locations and
63 socioeconomic conditions might be inadequate.

64 Many factors might influence the distribution of diseases at different spatial scales.
65 Climate might affect the spread of viruses given its known effect on biological processes that
66 influences many biogeographical patterns, including the distribution of diseases and human
67 behavior (e.g., Murray et al., 2018). Geographic distance represents the geographical space
68 where the disease spread following the distribution of hosts and has also ~~been found to~~ explain
69 biogeographic patterns (Pulin 2003, Nekola & White 2004, Warren 2014). Socioeconomic
70 characteristics of countries could be viewed as a proxy for the ability to identify and treat
71 infected people and for the governability necessary to make fast political decision and avoid the
72 spread of new diseases. Finally, the global transportation network might surpass other factors as
73 it can reduce the relative importance of geographic distance and facilitate the spread of viruses
74 and their vectors (Brockmann & Helbing 2013, Pybus et al., 2015). According to the
75 International Air Transport Association (2019) more than 4 billion passengers traveled abroad in
76 2018. This amount of travelers reaching most of our planet's surface represents a human niche
77 construction (~~i.e. global transportation network~~; Boivin et al., 2016) that facilitates the global
78 spread of viruses and vectors (Brockmann & Helbing 2013) in the same way it facilitated the
79 spread of invasive species and domesticated animals over modern human history (Boiving et al.,
80 2016).

81 The spread of SARS-CoV-2 from central China to other locations might be strongly
82 associated with inter-country connections, which might largely surpass the effect of climate
83 suitability. Thus, at this point of the pandemic, there is still a distributional disequilibrium that
84 can generate very biased predictions based on climatic correlative modeling (De Marco et al.,

85 2008). ~~Thus~~, here we used an alternative macroecological approach (Burnside et al., 2012), based
86 on the geographical patterns of exponential growth rates of the disease at country level, to
87 investigate variations ~~on~~ the growth rates of SARS-CoV-2. We studied the effect of
88 environment, socioeconomic ~~and~~ global transportation controlling for spatial autocorrelation that
89 could bias model significance. By analyzing these factors, we show that the exponential growth
90 of COVID-19 at global scale is explained mainly by country's importance in global
91 transportation network (~~i.e., air transportation~~).

92

93 **Material & Methods**

94 We collected the number of people infected by ~~the~~ COVID-19 per day from the John
95 Hopkins (Dong et al., 2020) and European Centre for Disease Prevention and Control (ECDC,
96 2020). ~~This data is~~ available for 204 countries, for which 65 had more than 100 cases recorded
97 and for which time series had at least 30 days after the 100th case. We also performed the
98 analysis considering countries with more than 50 cases, but it did not qualitatively change our
99 results. Thus, we only show the results for countries with more than 100 cases.

100 In our analysis, we only used the exponential portion of the time series data (i.e. number
101 of people infected per day) and excluded days after stabilization or decrease in total number of
102 cases. We empirically modelled each time series using an exponential growth model for each
103 country and calculated both the intrinsic growth rate (r) and the regression coefficient of the log
104 growth series to be used as the response variable in our models. **Because both were highly**
105 **correlated (Person's $r = 0.97$),** we used only the regression coefficient to represent the growth
106 rate of COVID-19 in our study.

107 To investigate potential correlates of the virus growth rate, we downloaded climatic and
108 socioeconomic data of each country. We used climatic data represented by monthly average
109 minimum and maximum temperature (°C) and total precipitation (mm) retrieved from the
110 WorldClim database (<https://www.worldclim.org>) (Fick & Hijmans 2017). We used monthly
111 available data for the most recent year available in WorldClim. We extracted climatic data from
112 the months of January, February, March, and December to represent the climatic conditions of
113 the winter season in the Northern Hemisphere and the summer season in the Southern
114 Hemisphere. From these data, we computed the mean value of climatic variables across each
115 country. Finally, minimum and maximum temperatures were combined to estimate monthly
116 mean temperature for December, January, February, and March, which was used in the model
117 along with total precipitation for the same months. However, using different combinations of
118 these variables (i.e., using means of minimum or maximum temperatures, as well as minimum or
119 maximum for each month) did not qualitatively affect our results.

120 We extracted socioeconomic data for each country. Human Development Index (HDI)
121 rank, mean number of school years in 2015, gross national income (GNI) per capita in 2011,
122 population size in 2015 and average annual population growth rate between 2010-2015 were
123 used in our study and downloaded from the United Nations database
124 (<http://hdr.undp.org/en/data>). We also obtained a mean value of health investment in each
125 country by averaging the annual health investments between 2005-2015 obtained from the World
126 Health Organization database (<http://apps.who.int/gho/data/node.home>). Due to the strong
127 collinearity among some of these predictors, HDI rank and mean number of school years were
128 removed from our final model.



129 Finally, we also downloaded air transportation data from the OpenFlights (2014) database
130 regarding the airports of the world, which informs where each airport is located including
131 country location (7,834 airports), and whether there is a direct flight connecting the airports
132 (67,663 connections). We checked the Openflights database to make the airports and connections
133 compatible by including missing or fixing airport codes and removing six unidentified airport
134 connections resulting in a total of 7,834 airports and 67,657 connections. We used this
135 information to build an air transportation network that reflects the existence of a direct flight
136 between the airports while considering the direction of the flight. Thus, the airport network is a
137 unipartite, binary, and directed graph where airports are nodes and flights are links (Fig 1, Fig
138 S1). In the following step, we collapsed the airports' network into a country-level network using
139 the country information to merge all the airports located in a country in a single node (e.g.,
140 United States had 613 airports that were merged in a single vertex representing the country). The
141 country-level network (Fig 1, Fig S1) is a directed weighted graph where the links are the
142 number of connections between 226 countries which is collapsed for the 65 countries that had
143 more than 100 cases and for which time series data had at least 30 days after the 100th case .
144 Afterward, we measured the countries centrality in the network using the Eigenvector Centrality
145 (Bonacich, 1987), ~~hereafter centrality~~, that weights the importance of a country in the network
146 considering the number of connections with other countries and how well connected these
147 countries are to other countries – indirect connections. All networks analyses were generated
148 using package *igraph* (Csardi & Nepusz, 2006).



149 We evaluated the relationship between the predictors (climatic, socioeconomic and
150 transport data) and our growth rate parameter using a standard multiple regression (OLS) after
151 ~~taking into consideration~~ the distribution of the original predictors as well as the normality of

152 ~~model~~ residuals. Moreover, OLS residuals were inspected to evaluate the existence of spatial
153 autocorrelation that could upward bias the significance of predictor variables on the model using
154 Moran's I correlograms (Legendre & Legendre 2013). Prior to the analysis, we applied
155 logarithmic (mean precipitation, total population size, and network centrality) and square root
156 (mean health investments) transformations to the data to approximate a normal distribution.

157

158 **Results**

159 The models used to estimate COVID-19 growth rate on different countries showed an
160 average R^2 of 0.91 (SD = 0.04), varying from 0.78 to 0.99, indicating an overall excellent
161 performance on estimating growth rates. The geographical patterns in the growth rates of
162 COVID-19 cases do not show a clear trend, at least in terms of latitudinal variation, that would
163 suggest a climatic effect at macroecological scale (Fig. 2A).

164 We build one model including only climate and socioeconomic variables, which
165 explained *only 14%* of the variation on growth rates. This model did not have spatial
166 autocorrelation in the residuals. When we added country centrality (i.e. country importance in
167 global transportation network) as a predictor, the R^2 increased to 48.6%. In this model, annual
168 population growth and precipitation had positive and significant effects (Table 1, ~~$P=0.036$~~ , ~~P~~
169 ~~$=0.041$~~ , Fig 2), while health investments had a negative and significant effect on growth rate
170 (Table 1, ~~$P=0.035$~~ , Fig 2). Here, exponential growth rates increased *strongly* in response to
171 countries importance in the transportation network which has more than two times the effect size
172 of any significant variable (Table 1). However, it is also important to note that growth rates of
173 COVID-19 weakly increases with increases of annual population growth and precipitation, and

174 decreases with higher investments in health (Table 1). Statistical coefficients were not upward
175 biased by spatial autocorrelation.

176

177 Discussion

178 ~~The pandemic state of SARS-CoV-2 is killing hundreds of thousands of people, put the~~
179 ~~world in quarantine and is causing an unprecedented economic crisis. The rates of increase of~~
180 ~~new cases of COVID-19 is faster in some countries than others. To understand why growth rates~~
181 ~~are different among countries we investigate the effect of climatic, socioeconomical and human~~
182 ~~transportation variables that could have important roles on the exponential phase of COVID-19.~~
183 At global scale, temperature, population size and Gross National Income had no significant
184 effect on the exponential phase of COVID-19. However, annual population growth, health
185 investments and precipitation show significant, but weak effects on growth rates. Countries'
186 importance in the global transportation network has a key role on the severity of COVID-19
187 pandemic in different countries as it is strongly associated with the growth rates of the disease
188 (Fig 2).

189 The centrality measure is widely used to discover distinguished nodes on ~~many~~ networks,
190 including epidemiological networks (e.g., Madotto & Liu 2016). Our findings reinforce the
191 importance of propagule pressure on disease dissemination (Tian et al., 2017, Chinazzi et al.,
192 2020). Aerial transportation is an important predictor of COVID-19 dissemination in China
193 (Kraemer et al., 2020), in Brazil (Ribeiro et al., 2020), and in Mexico (Dáttillo et al., 2020). It is
194 quite likely that further phases of COVID-19 spread, in terms of peak of infections and decrease
195 in mortality rates, will be better related to socioeconomics characteristics of each county and
196 their political decisions when secondary transmissions were identified. **We can already clearly**

197 identify the effects of adopting strong social isolation policies in China (see Kraemer et al.,
198 2020) and, on the opposite side of this spectrum, in European countries like Italy, Spain and
199 England (Enserink & Kupfershmidt 2020). Our analyses call attention to the case of Brazil, a
200 well-connected tropical country that presents one of the highest increase rates of COVID-19 in
201 the tropics in its exponential phase (Fig 2A). If decision makers ~~take into consideration~~, yet
202 unsupported claims that growth rates of COVID-19 in its exponential phase might be lower in
203 warmer and humid countries, we might observe terrible scenarios unrolling in tropical countries,
204 especially in those with limited health care structure, such as Brazil. As our results also show,
205 those countries that invested less in health are also the ones with faster growth rates of covid-19
206 in its exponential phase (Fig 2, Table 1).

207 When discussing and modelling the effect of climate on SARS CoV-2 it is important to
208 remember that modern human society is a complex system composed of strongly connected
209 societies that are all susceptible to rare events. It is also critical to consider the negative
210 correlations between climate and local or regional socioeconomic conditions (i.e., inadequate
211 sanitary conditions and poor nutritional conditions) that could easily counteract any potential
212 climatic effect at local scales, such as lower survival rates of viruses exposed to high humidity,
213 temperatures and high UV irradiation (Wang et al., 2020, Duan et al., 2003). Tropical regions
214 will experience mild climate conditions in a couple of months. Thus, regardless of the influence
215 of local environmental conditions, tropical countries could still expect high contagious rates. In
216 addition, our results points to a positive effect of precipitation on growth rates, which is the
217 contrary of what has been suggested by climate suitability models. Finally, climatic suitability
218 models might be ephemeral for very mathematized modelling fields of science such as
219 epidemiology and virology that developed over time very realistic models that enables the

220 possibility of learning with parameters of similar viruses (i.e. SARS) that can definitely help and
221 instruct decision makers to take actions before it is too late.

222 Here we showed that countries' importance in the global transportation network has a key
223 role on COVID-19 growth rates in its exponential phase. Our results reinforce board control
224 measures in international airports (Bitar et al., 2009, Nishiura & Kamiya 2011) during
225 exceedingly early stages of pandemics to prevent secondary transmissions that could lead to
226 undesired scenarios of rapid synchronically spread of infectious diseases in different countries.
227 The rapid international spread of the severe acute respiratory syndrome (SARS) from 2002 to
228 2003 led to extensively assessing entry screening measures at international borders of some
229 countries (Bell et al., 2003, John et al., 2017). The 2019-2020 world spread of COVID-19
230 highlights that improvements and testing of board control measures (i.e. screening associated
231 with fast testing and quarantine of infected travellers) might be a cheap solution for humanity in
232 comparison to health systems breakdowns and unprecedented global economic crises that the
233 spread of infectious disease can cause. However, it is important to note that board control of
234 potentially infected travellers and how to effectively identify them is still a hotly debated topic in
235 epidemiology and there is still no consensus on accurate methodologies for its application (Sun
236 et al., 2017).

237

238 **Conclusions**

239 Here, we show that countries' importance in the global transportation network has a key
240 role on the severity of COVID-19 pandemic in different countries as it is strongly associated
241 with the growth rates of the disease (Fig 2). We do not expect that our results using a
242 macroecological approach at a global scale would have a definitive effect on decision-making in

243 terms of public health in any particular country, province, or city. However, we expect that our
244 analyses show that current claims that growth of COVID-19 pandemics may be lower in
245 developing tropical countries should be taken very carefully, at risk to disturb well-established
246 and effective policy of social isolation that may help to avoid higher mortality rates due to
247 collapse in national health systems.

248

249 **Acknowledgments**

250 This paper was developed in the context of the human macroecology project on the National
251 Institute of Science and Technology (INCT) in Ecology, Evolution and Biodiversity
252 Conservation, supported by CNPq (grant 465610/2014-5) and FAPEG (grant
253 201810267000023). JAFDF, RD, LCT are also supported by CNPq productivity scholarships.
254 We thank Thiago F. Rangel, André Menegotto, Robert D. Morris and Marcus Cianciaruso for
255 their constructive comments on early version of the manuscript.

256

257

258 **References**

- 259 Araujo MB, Naimi B. 2020 Spread of SARS-CoV-2 Coronavirus likely to be constrained by
260 climate. *medRxiv*, 2020.03.12.20034728. (doi:10.1101/2020.03.12.20034728)
261
- 262 Barreca AI, Shimshack JP. 2012 Absolute humidity, temperature, and influenza mortality: 30
263 years of county-level evidence from the united states. *Am. J. Epidemiol.* **176**, 114–122.
264 (doi:10.1093/aje/kws259)
265
- 266 Bell DM *et al.* 2004 Public health interventions and SARS spread, 2003. *Emerg. Infect. Dis.* **10**,
267 1900–1906. (doi:10.3201/eid1011.040729)
268
- 269 Biggerstaff M, Cauchemez S, Reed C, Gambhir M, Finelli L. 2014 Estimates of the reproduction
270 number for seasonal, pandemic, and zoonotic influenza: A systematic review of the
271 literature. *BMC Infect. Dis.* **14**, 1–20. (doi:10.1186/1471-2334-14-480)
272

- 273 Bitar D. , Goubar A. DJC. 2009 International travels and fever screening during epidemics: a
274 literature review on the effectiveness and potential use of non-contact infrared
275 thermometers. *Euro Surveill* **14**, pii=19115.
276
- 277 Boivin NL, Zeder MA, Fuller DQ, Crowther A, Larson G, Erlandson JM, Denhami T, Petraglia
278 MD. 2016 Ecological consequences of human niche construction: Examining long-term
279 anthropogenic shaping of global species distributions. *Proc. Natl. Acad. Sci. U. S. A.* **113**,
280 6388–6396. (doi:10.1073/pnas.1525200113)
281
- 282 Bonacich P. 1987 Power and Centrality: A Family of Measures. *Am. J. Sociol.* **92**, 1170–1182.
283 (doi:10.1086/228631)
- 284 Brockmann D, Helbing D. 2013 The hidden geometry of complex, network-driven contagion
285 phenomena. *Science (80)*. **342**, 1337–1342. (doi:10.1126/science.1245200)
286
- 287 Burnside WR, Brown JH, Burger O, Hamilton MJ, Moses M, Bettencourt LMA. 2012 Human
288 macroecology: linking pattern and process in big-picture human ecology. *Biol. Rev.* **87**,
289 194–208. (doi:10.1111/j.1469-185X.2011.00192.x)
290
- 291 Chan KH, Peiris JSM, Lam SY, Poon LLM, Yuen KY, Seto WH. 2011 The effects of
292 temperature and relative humidity on the viability of the SARS coronavirus. *Adv. Virol.*
293 **2011**. (doi:10.1155/2011/734690)
294
- 295 Chinazzi M *et al.* 2020 The effect of travel restrictions on the spread of the 2019 novel
296 coronavirus (COVID-19) outbreak. *Science* **9757**, 1–12. (doi:10.1126/science.aba9757)
297
- 298 Chipperfield JD. 2020 On the inadequacy of species distribution models for modelling the spread
299 of SARS-CoV-2 : response to Araújo and Naimi. *ecoRxiv*
300
- 301 Csardi G, Nepusz T .2006. The igraph software package for complex network
302 research. *InterJournal*, **Complex Systems**, 1695. <http://igraph.org>.
303
- 304 Dattilo W, Silva AC, Guevara R, McGregor-Fors I, Pontes S. 2020 COVID-19 most vulnerable
305 Mexican cities lack the public health infrastructure to face the pandemic: a new
306 temporally-explicit model. *medRxiv* , 1–13. (doi:10.1101/2020.04.10.20061192)
307
- 308 De Marco P, Diniz-Filho JAF, Bini LM. 2008 Spatial analysis improves species distribution
309 modelling during range expansion. *Biol. Lett.* **4**, 577–580. (doi:10.1098/rsbl.2008.0210)
310
- 311 Delamater PL, Street EJ, Leslie TF, Yang YT, Jacobsen KH. 2019 Complexity of the basic
312 reproduction number (R0). *Emerg. Infect. Dis.* **25**, 1–4. (doi:10.3201/eid2501.171901)
313
- 314 Dong E, Du H, Gardner L. 2020 An interactive web-based dashboard to track COVID-19 in real
315 time. *Lancet Infect. Dis.* **20**, 533–534. (doi:10.1016/S1473-3099(20)30120-1)
316

- 317 Doremalen NV, Bushmaker T, Munster VJ. 2013 Stability of middle east respiratory syndrome
318 coronavirus (MERS-CoV) under different environmental conditions. *Eurosurveillance*
319 **18**, 1–4. (doi:10.2807/1560-7917.ES2013.18.38.20590)
320
- 321 Duan S-M *et al.* 2003 Stability of SARS coronavirus in human specimens and environment and
322 its sensitivity to heating and UV irradiation. *Biomed. Environ. Sci.* **16**, 246–255.
323
- 324 Enserink, M & Kupferschmidt, K. (2020). Mathematics of life and death: How disease models
325 shape national shutdowns and other pandemic policies. *Science*
326 ([https://www.sciencemag.org/news/2020/03/mathematics-life-and-death-how-disease-](https://www.sciencemag.org/news/2020/03/mathematics-life-and-death-how-disease-models-shape-national-shutdowns-and-other#)
327 [models-shape-national-shutdowns-and-other#](https://www.sciencemag.org/news/2020/03/mathematics-life-and-death-how-disease-models-shape-national-shutdowns-and-other#))
328
- 329 European Centre for Disease Prevention and Control (ECDC). COVID-19 - Situation update –
330 worldwide. Stockholm: ECDC; 1 Apr 2020. Available from:
331 <https://www.ecdc.europa.eu/en/geographical-distribution-2019-ncov-cases>
332
- 333 Fick SE, Hijmans RJ. 2017 WorldClim 2: new 1-km spatial resolution climate surfaces for global
334 land areas. *Int. J. Climatol.* **37**, 4302–4315. (doi:10.1002/joc.5086)
335
- 336 Gaunt ER, Hardie A, Claas ECJ, Simmonds P, Templeton KE. 2010 Epidemiology and clinical
337 presentations of the four human coronaviruses 229E, HKU1, NL63, and OC43 detected
338 over 3 years using a novel multiplex real-time PCR method. *J. Clin. Microbiol.* **48**, 2940–
339 2947. (doi:10.1128/JCM.00636-10)
340
- 341 Harris I, Jones PD, Osborn TJ, Lister DH. 2014 Updated high-resolution grids of monthly
342 climatic observations - the CRU TS3.10 Dataset. *Int. J. Climatol.* **34**, 623–642.
343 (doi:10.1002/joc.3711)
344
- 345 International Air Transport Association. 2019. Annual
346 Review([https://www.iata.org/contentassets/c81222d96c9a4e0bb4ff6ced0126f0bb/iata-](https://www.iata.org/contentassets/c81222d96c9a4e0bb4ff6ced0126f0bb/iata-annual-review-2019.pdf)
347 [annual-review-2019.pdf](https://www.iata.org/contentassets/c81222d96c9a4e0bb4ff6ced0126f0bb/iata-annual-review-2019.pdf))
348
- 349 John St. RK, King A, De Jong D, Bodie-Collins M, Squires SG, Tam TWS. 2005 Border
350 screening for SARS. *Emerg. Infect. Dis.* **11**, 6–10. (doi:10.3201/eid1101.040835)
351
- 352 Kraemer MUG *et al.* 2020 The effect of human mobility and control measures on the COVID-19
353 epidemic in China. *Science* **497**, 493–497. (doi:10.1126/science.abb4218)
354
- 355 Legendre P, Lensedre L. Numerical Ecology. Elsevier Science.
356
- 357 Lowen AC, Mubareka S, Steel J, Palese P. 2007 Influenza virus transmission is dependent on
358 relative humidity and temperature. *PLoS Pathog.* **3**, 1470–1476.
359 (doi:10.1371/journal.ppat.0030151)

- 360
361 Madotto A, Liu J. 2016 Super-Spreader Identification Using Meta-Centrality. *Sci. Rep.* **6**, 1–10.
362 (doi:10.1038/srep38994)
363
- 364 Murray KA, Olivero J, Roche B, Tiedt S, Guégan JF. 2018 Pathogeography: leveraging the
365 biogeography of human infectious diseases for global health management. *Ecography*
366 (*Cop.*) **41**, 1411–1427. (doi:10.1111/ecog.03625)
367
- 368 Nekola JC, White PS. 1999 The distance decay of similarity in biogeography and ecology. *J.*
369 *Biogeogr.* **26**, 867–878. (doi:10.1046/j.1365-2699.1999.00305.x)
370
- 371 Nishiura H, Kamiya K. 2011 Fever screening during the influenza (H1N1-2009) pandemic at
372 Narita International Airport, Japan. *BMC Infect. Dis.* **11**, 1–11. (doi:10.1186/1471-2334-
373 11-111)
374
- 375 Openflights.org database. 2014. <http://openflights.org/data.html>. Accessed 20 March 2020
- 376 Poulin R. 2003 The decay of similarity with geographical distance in parasite communities of
377 vertebrate hosts. *J. Biogeogr.* **30**, 1609–1615. (doi:10.1046/j.1365-2699.2003.00949.x)
378
- 379 Pybus OG, Tatem AJ, Lemey P. 2015 Virus evolution and transmission in an ever more
380 connected world. *Proc. R. Soc. B Biol. Sci.* **282**, 1–10. (doi:10.1098/rspb.2014.2878)
381
- 382 Ribeiro SP *et al.* 2020 Severe airport sanitarian control could slow down the spreading of
383 COVID-19 pandemics in Brazil. *medRxiv*, 2020.03.26.20044370.
384 (doi:10.1101/2020.03.26.20044370)
385
- 386 Sajadi MM, Habibzadeh P, Vintzileos A, Shokouhi S, Miralles-Wilhelm F, Amoroso A. 2020
387 Temperature and Latitude Analysis to Predict Potential Spread and Seasonality for
388 COVID-19. *SSRN Electron. J.*, 6–7. (doi:10.2139/ssrn.3550308)
389
- 390 Shaman J, Pitzer VE, Viboud C, Grenfell BT, Lipsitch M. 2010 Absolute humidity and the
391 seasonal onset of influenza in the continental United States. *PLoS Biol.* **8**.
392 (doi:10.1371/journal.pbio.1000316)
393
- 394 Sun G., Matsui T., Kirimoto T., Yao Y., Abe S. .2017. Applications of Infrared Thermography
395 for Noncontact and Noninvasive Mass Screening of Febrile International Travelers at
396 Airport Quarantine Stations. In: Ng E., Etehadtavakol M. (eds) *Application of Infrared to*
397 *Biomedical Sciences*. Series in BioEngineering. Springer, Singapore
398
- 399 Tan J, Mu L, Huang J, Yu S, Chen B, Yin J. 2005 An initial investigation of the association
400 between the SARS outbreak and weather: With the view of the environmental
401 temperature and its variation. *J. Epidemiol. Community Health* **59**, 186–192.
402 (doi:10.1136/jech.2004.020180)
403

- 404 Tian H *et al.* 2017 Increasing airline travel may facilitate co-circulation of multiple dengue virus
405 serotypes in Asia. *PLoS Negl. Trop. Dis.* **11**, 1–15. (doi:10.1371/journal.pntd.0005694)
406
- 407 Wang J, Tang K, Feng K, Lv W. 2020 High Temperature and High Humidity Reduce the
408 Transmission of COVID-19. *SSRN Electron. J.* , 1–19. (doi:10.2139/ssrn.3551767)
409
- 410 Warren DL, Cardillo M, Rosauer DF, Bolnick DI. 2014 Mistaking geography for biology:
411 inferring processes from species distributions. *Trends Ecol. & Evol.* **29**, 572–580.
412 (doi:10.1016/j.tree.2014.08.003)
413
- 414 World Health Organization. 2020. Statement on the meeting of the International Health
415 Regulations (2005) *Emergency Committee regarding the outbreak of novel coronavirus*
416 *(2019-nCoV)*. Retrieved from [https://www.who.int/news-room/detail/23-01-2020-
417 statement-on-the-meeting-of-the-international-health-regulations-\(2005\)-emergency-
418 committee-regarding-the-outbreak-of-novel-coronavirus-\(2019-ncov\)](https://www.who.int/news-room/detail/23-01-2020-statement-on-the-meeting-of-the-international-health-regulations-(2005)-emergency-committee-regarding-the-outbreak-of-novel-coronavirus-(2019-ncov))
419
- 420 Zuk T, Rakowski F, Radomski JP. 2009 Probabilistic model of influenza virus transmissibility at
421 various temperature and humidity conditions. *Comput. Biol. Chem.* **33**, 339–343.
422 (doi:10.1016/j.compbiolchem.2009.07.005)
423
- 424

Figure 1

Air transportation network

Fig 1. Air transportation network among 65 countries that had more than 100 cases and for which time series data had at least 30 days after the 100th case. Different colours represent modules of countries that are more connected to each other. Different sizes of each node represent the growth rate of COVID-19 estimated for each country (See results Fig 2).

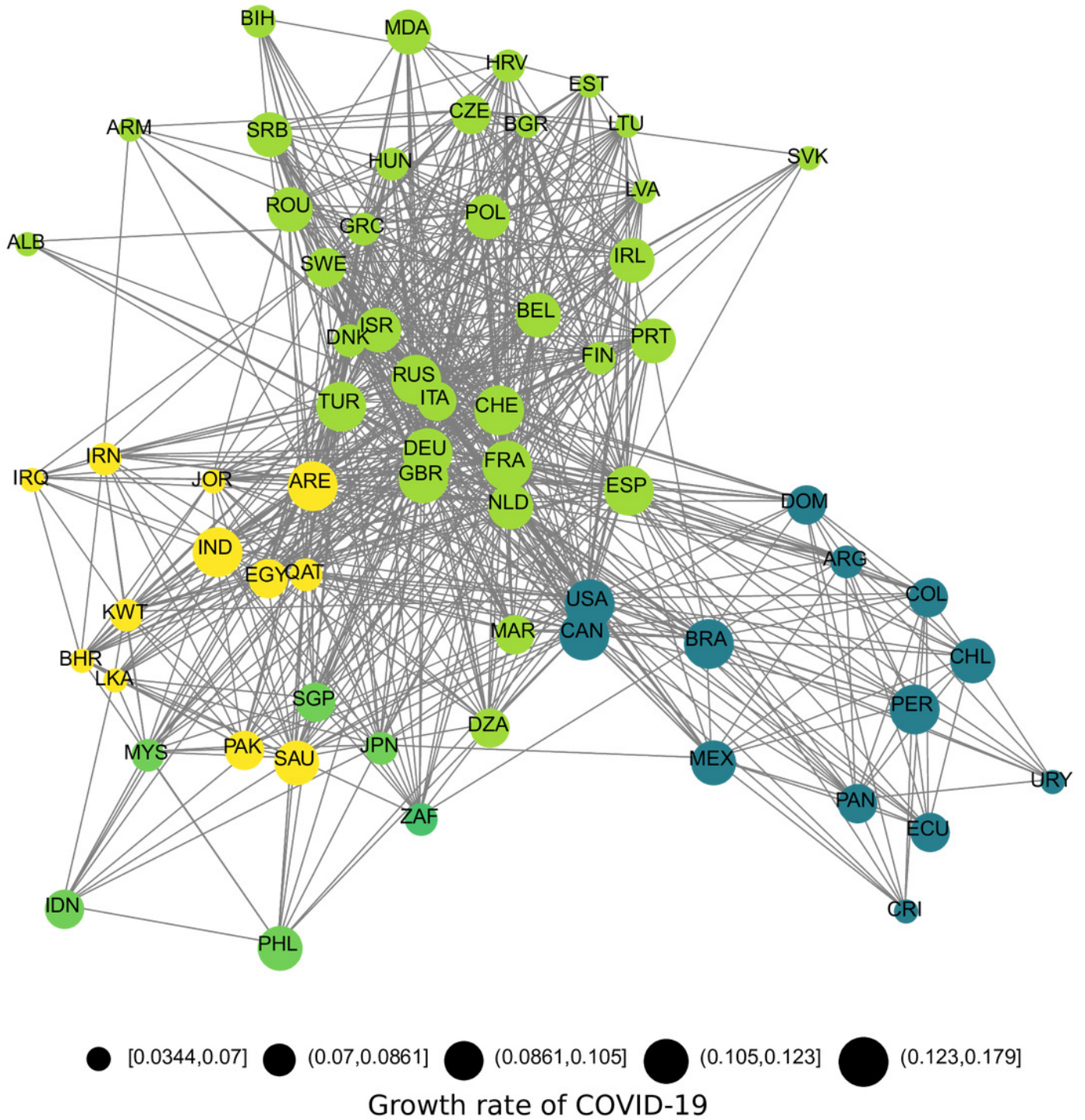


Figure 2

Geographical patterns of response and significant predictor variables

Fig 2. Geographical patterns of growth rate of covid-19 in the exponential phase (**A**), the Eigenvector Centrality that represents countries' importance in global transportation network (**B**), Annual population growth (**C**), health investments (**D**) and mean precipitation (**E**). The relationship between growth rate and the log transformed eigenvector centrality is showed in **F**. **G**, **H** and **I** are partial plots showing the relationship between the residuals of growth rates vs log transformed eigenvector centrality and annual population growth, health investments and mean precipitation.

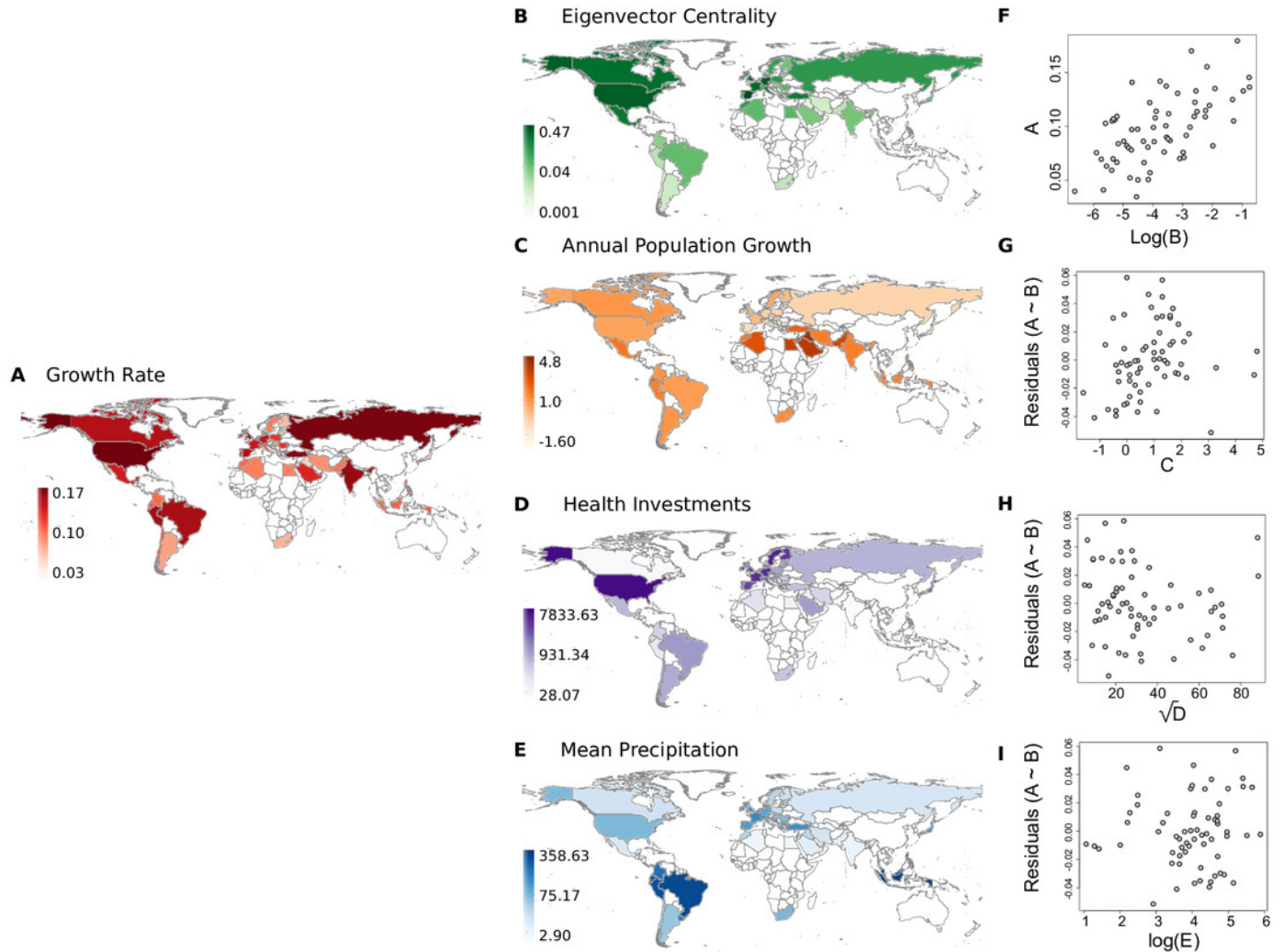


Table 1 (on next page)

Model Statistics

Table 1. Model statistics for all variables used in the study.

1 **Table 1.** Model statistics for all variables used in the study.

	Standardized				
	Estimate	Estimate	Std Error	t value	P-value
<i>Intercept</i>		0.149	0.026	3.547	< 0.001
<i>Eigenvector Centrality</i>	0.758	0.016	0.002	6.124	< 0.001
<i>Gross National Income</i>	0.16	0.000	0.000	1.491	0.141
<i>Population Size</i>	-0.096	-0.004	0.004	-0.953	0.344
<i>Annual population growth</i>	0.306	0.008	0.003	2.139	0.036
<i>Health investment</i>	-0.287	-0.0004	0.000	-2.155	0.035
<i>Mean Temperature</i>	-0.127	-0.0003	0.000	-0.908	0.367
<i>Mean Precipitation</i>	0.253	0.007	0.003	2.091	0.041

2

3